

INFLUENCE OF INTRACELLULAR DELAY ON THE DYNAMICS OF HEPATITIS C VIRUS

SANDIP BANERJEE*, RAM KEVAL†, AND SUNITA GAKKHAR‡

Abstract. In this paper we present a delay induced model for hepatitis C virus incorporating the healthy and infected hepatocytes as well as infectious and noninfectious virions. The model is mathematically analyzed and characterized, both for the steady states and the dynamical behavior of the model. It is shown that time delay does not affect the local asymptotic stability of the uninfected steady state. However, it can destabilize the endemic equilibrium, leading to Hopf bifurcation to periodic solutions with realistic data sets. The model is also validated using 12 patient data obtained from the study, conducted at the University of Sao Paulo Hospital das clinicas.

Key words. Hepatitis C virus, Intracellular delay, Stability analysis, Bifurcation analysis.

AMS subject classifications. 92B99

1. Introduction. An overwhelming number of people globally are infected with the hepatitis C virus (HCV). Chronic HCV often requires treatment in the form of liver transplant [14]. Unfortunately, most of the cases of chronic HCV lead to fatalities. The traditional treatment with pegylated interferon (IFN) has met with moderate success. The current front line therapy for HCV involves a combination of IFN and ribavirin [14, 18]. Even then this combination therapy elicits success in about half of the treated cases [14] and is quite expensive. It is therefore imperative to study the mechanism of viral dynamics and the precise extent of therapeutic response. The eventual goal would be to improve upon the therapeutic protocols [18] keeping in mind the goal of minimizing the viral load while also minimizing the toxic side effects [6]. As already pointed out the therapeutic effectiveness of IFN is moderate but patients show remarkable progress when it is combined with ribavirin [18, 21]. The response to the combination therapy has been varied in nature [14, 18]. In some cases, there has been a sustained fall of the virus below detection levels, whereas in other cases there has either been a fall in the viral load followed by a relapse after cession of treatment as well as cases of complete non response [14, 18]. Even in successful cases, the viral load has exhibited biphasic and triphasic levels of decline [10].

Mathematical models which are simple but elegant have played a pivotal role (especially in recent years) in the understanding of the mechanism of viral dynamics in the cases of influenza, hepatitis B and human immunodeficiency virus (HIV) [17, 30, 32, 1, 27]. One of the earliest realistic model to reflect the viral dynamics of HCV was a work by Neumann et al. that appeared in 1998 [29]. The model [29] comprised of a simple but coupled system of three ordinary differential equations (ODEs). It involved the mechanism of the uninfected and the productively infected target cells (which in case of HCV are the hepatocytes). The treatment involved only IFN and did not include ribavirin. The hepatocytes were assumed to have a constant source of supply and undergo a natural death. Some of these hepatocytes were rendered into an infected state by the HCV resulting in infected hepatocytes, some of which

*Department of Mathematics, Indian Institute of Technology Roorkee, Roorkee, Uttarakhand, 247667, India (sandofma@iitr.ac.in).

†Department of Mathematics, Indian Institute of Technology Roorkee, Roorkee, Uttarakhand, 247667, India (ramkeval@gmail.com).

‡Department of Mathematics, Indian Institute of Technology Roorkee, Roorkee, Uttarakhand, 247667, India (sungkma@iitr.ac.in).

were lost due to immune response. The virions were following a birth (due to infected hepatocytes) and a natural death process [14]. The authors then incorporated into the model the effectiveness of IFN on the viral load. It was observed that the IFN was primarily playing the role of rendering the virions ineffective, while having a minimal role in controlling the transition of hepatocytes from an uninfected to an infected state. An assumption in the contrary to the previous statement, resulted in the model showing results of a single phase delay which contradicted the clinical results. However, when the assumption of IFN being mainly used to target the virus, was used in the model, the results showed a close matching with the experimental results [21, 29] of biphasic decline in the viral load. Once this model was validated for *in vivo* HCV dynamics it was used to estimate key parameter values of the model. The drawback of this model was its inability to capture the long-term behavior of dynamics as well as its failure to take into account the consequences of usage of ribavirin.

The motivation of a subsequent work was to address the issues that were left open for deliberations in [29]. Dixit et al. [15], in an endeavor to capture the effects of ribavirin in the dynamics, presented an improved model. In this model the presence of ribavirin created two categories of viruses (one infectious and the other noninfectious) owing to the understanding that the predominant role of ribavirin was to render a fraction of the virus into a noninfectious state. The most interesting finding of this work was the observation in numerical simulations that ribavirin has a little role to play in the first phase of a biphasic decline of viral load. It also affects the second phase and that too only when the effectiveness of IFN is moderate. The biological explanation of this as provided by the authors [15] is that when IFN is effective, it can control the virions and hence ribavirin is left with a little role to play. It is when IFN is minimally effective that ribavirin reduces the viral load not by arresting the virus which in turn would have affected the production of infected hepatocytes, but because of the fact that viruses have been rendered noninfectious [14]. This model was also successful in capturing some of the long-term effects.

While both these models [29, 15] are widely regarded as seminal work in mathematical modeling of HCV dynamics, they did not fully address the clinical observations of triphasic decline and more importantly, the critical issue of non-response (which unfortunately happens in a majority of the chronic cases). These limitations of [29, 15] were addressed in a recent work by Dahari et al. [10]. This model was an extension of the previous models [29, 15]. The model for the first time included the mechanism of the liver by including a logistic growth term for the hepatocytes (both uninfected and infected) and a maximum carrying capacity which put a limit on the proliferation of hepatocytes. They were able to obtain an elegant, yet simple critical effectiveness threshold beyond which one cannot attain sustained long time viral decay. This threshold which was a function of both viral and host parameters, was able to explain the rationale being the non-effectiveness of the treatment. This homeostatic cell proliferation terms were also able to address mathematically the causes behind the triphasic decline observed in some patients. This model, however, still has aspects that have to be addressed in terms of clinical validation, since the estimation of parameters from liver mechanism still remains a gray area. A similar model has been proposed by Banerjee et al. [2], where dynamical behavior of the HCV due to separate efficacies of interferon and ribavirin hold the key factor.

Time delays in connection with viral dynamics, namely, HIV, Lymphocytic choriomeningitis virus (LCMV), Hepatitis B are always an interesting features of study

among the researches as models of viral infection dynamics with delays may have complicated impact on the dynamics of a system. Also, a delay in the viral production of infected cells may drastically change the estimates of viral clearance [28]. Delay may cause the loss of stability and can bifurcate various periodic solutions [20]. Clearly in viral dynamics, the time for viral infection is not instantaneous. Development of the mathematical model and the associated analytical and numerical techniques that incorporate discrete time delay into the model of hepatitis C viral dynamics is the primary motivation here.

Section 2 gives the formulation of the model in details. Section 3 deals with the linear stability analysis and bifurcation analysis, including the estimation of the length of delay to preserve stability, direction and stability of Hopf bifurcation. Section 4 gives the numerical results and its biological implications and the paper ends with a discussion.

2. Model Formulation. The proposed model is the amalgamation and modification of the models that appear in [6, 2], which is represented by the system of coupled ODEs:

$$\begin{aligned}
 \frac{dT}{dt} &= s + rT \left(1 - \frac{T+I}{T_{\max}} \right) - d_1T - (1 - c\eta_1)\alpha V_I T, \\
 \frac{dI}{dt} &= (1 - c\eta_1)\alpha V_I T - d_2I, \\
 \frac{dV_I}{dt} &= \left(1 - \frac{\eta_r + \eta_1}{2} \right) \beta I - d_3V_I, \\
 \frac{dV_{NI}}{dt} &= \left(\frac{\eta_r + \eta_1}{2} \right) \beta I - d_3V_{NI}.
 \end{aligned}
 \tag{2.1}$$

Here, T denotes the target cells (uninfected hepatocytes), I are infected hepatocytes (productively infected cells), V_I and V_{NI} represent the infectious and non-infectious viruses (virions) respectively. The first equation projects the growth of uninfected hepatocytes from a constant source at a rate s , followed by an intrinsic logistic growth term at a rate r . Please note that the logistic part is of the form $rT(1 - (T+I)/T_{\max})$, where T_{\max} is the carrying capacity of the hepatocytes (both infected as well as uninfected). This is because of the fact that as the threshold value T_{\max} is attained, the infected and the non-infected hepatocytes are not differentiated but considered as a whole. As already pointed out in [10], the logistic term is incorporated to capture the homeostatic cell proliferation. There are two drugs acting on the system, namely, interferon and ribavirin. At this point we note that η_1 is the efficacy of interferon in blocking the release of new virions. The term $(1 - c\eta_1)$ ($0 < c < 1$) reflects the ineffectiveness of interferon (which is much smaller than its effectiveness in blocking the virions and which is why we take $(0 < c < 1)$) in inhibiting hepatocytes conversion from the uninfected to the infected one.

The second equation gives the dynamics of infectious hepatocytes, where the uninfected hepatocytes (T) are infected by the infectious virions (V_I) at the rate α and the whole term $(1 - c\eta_1)\alpha V_I T$ shifts from the uninfected class to the infected one; $(-d_2I)$ is the natural death of the infected hepatocytes (I).

The combined effect of the interferon and ribavirin has been incorporated in the last two equations. Due to the combined efficacy, the infectious hepatocytes replicates into infectious (V_I) as well as non-infectious (V_{NI}) virions. The term $(1 - (\eta_r + \eta_1)/2)\beta I$ determines the growth of infectious virions due to non-efficacy of the combined drugs:

interferon and ribavirin, due to which the infected cells are replicating virions at a rate β . But, due the efficacy of the combined effect of interferon and ribavirin, the infected cells are replicating non-infectious virions at a rate β , which is given by the term $((\eta_r + \eta_1)/2)\beta I$, which also points out that the combined effect of the drugs interferon and ribavirin are successful in rendering the virions from an infected state to an uninfected one. Finally, the infectious and noninfectious viruses are assumed to have the same natural death rate of d_3 . Note that here $0 < \eta_1 < 1$ and $0 < \eta_r < 1$ lead to $0 < ((\eta_r + \eta_1)/2) < 1$.

It has been almost invariably observed that in viral dynamics, there is a time delay (say, τ) in conversion of the target cells (the CD4 T-cells in case of HIV [28] and hepatitis B viral dynamics [20] for instance) from an uninfected to an infected stage. This delay in transformation induces delay in the growth of infected cells. Hence, the model, which is represented by a system of coupled ODEs (equation(2.1)) is converted to a system of delay differential equations (DDEs):

$$\begin{aligned}
 \frac{dT}{dt} &= s + rT \left(1 - \frac{T+I}{T_{\max}}\right) - d_1T - (1 - c\eta_1)\alpha V_I T, \\
 \frac{dI}{dt} &= (1 - c\eta_1)\alpha V_I(t - \tau)T(t - \tau) - d_2I, \\
 \frac{dV_I}{dt} &= \left(1 - \frac{\eta_r + \eta_1}{2}\right)\beta I - d_3V_I, \\
 \frac{dV_{NI}}{dt} &= \left(\frac{\eta_r + \eta_1}{2}\right)\beta I - d_3V_{NI}.
 \end{aligned}
 \tag{2.2}$$

The system is subjected to initial conditions:

$$\begin{aligned}
 T(\theta) &= \psi_1(\theta), \quad I(\theta) = \psi_2(\theta), \quad V_I(\theta) = \psi_3(\theta), \quad V_{NI}(\theta) = \psi_4(\theta), \quad \theta \in [-\tau, 0], \\
 \psi_i(0) &\geq 0, \quad i = 1, 2, 3, 4
 \end{aligned}
 \tag{2.3}$$

where $(\psi_1(\theta), \psi_2(\theta), \psi_3(\theta), \psi_4(\theta)) \in C([- \tau, 0], R_{+0}^4)$, the Banach space of continuous functions, mapping the interval $[-\tau, 0]$ into R_{+0}^4 . We define R_{+0}^4 and R_+^4 (the interior of R_{+0}^4) as:

$$\begin{aligned}
 R_{+0}^4 &= ((T, I, V_I, V_{NI}) : T, I, V_I, V_{NI} \geq 0) \\
 R_+^4 &= ((T, I, V_I, V_{NI}) : T, I, V_I, V_{NI} > 0)
 \end{aligned}$$

This model of DDEs will form the fundamental mathematical framework for this paper.

3. Qualitative analysis of the model.

3.1. Equilibria and linear stability analysis. There exit two positive equilibrium points of (2.1), namely,

1. E_1 :

$$\hat{T} = \frac{T_{\max}}{2r} \left[(r - d_1) + \sqrt{(r - d_1)^2 + \frac{4rs}{T_{\max}}} \right], \quad r > d_1, \quad I = 0, \quad V_I = 0, \quad V_{NI} = 0.$$

2. E_2 :

$$T^* = \frac{d_2 d_3}{(1 - c\eta_1) \left(1 - \frac{\eta_r + \eta_1}{2}\right) \alpha \beta}, \quad I^* = \left(\frac{s R_0 T_{\max} + r \hat{T}^2}{r \hat{T} + d_2 R_0 T_{\max}} \right) \left(1 - \frac{1}{R_0} \right),$$

$$V_I^* = \left(1 - \frac{\eta_r + \eta_1}{2}\right) \frac{\beta I^*}{d_3}, \quad V_{NI}^* = \left(\frac{\eta_r + \eta_1}{2}\right) \frac{\beta I^*}{d_3}.$$

Here $R_0 = \frac{\hat{T}}{T^*}$ is the basic reproduction number. E_2 exists if $R_0 > 1$. We assume that $s \leq d_1 T_{\max}$, so that the model is physiologically realistic.

The characteristic equation about any equilibrium point $\bar{E}(\bar{T}, \bar{I}, \bar{V}_I, \bar{V}_{NI})$ is given by

$$(3.1) \quad \begin{vmatrix} r - d_1 - \frac{2r\bar{T}}{T_{\max}} - \frac{r\bar{I}}{T_{\max}} - (1 - c\eta_1)\alpha\bar{V}_I - \lambda & -\frac{r\bar{T}}{T_{\max}} & -(1 - c\eta_1)\alpha\bar{T} & 0 \\ (1 - c\eta_1)\alpha\bar{V}_I e^{-\lambda\tau} & -d_2 - \lambda & (1 - c\eta_1)\alpha\bar{T} e^{-\lambda\tau} & 0 \\ 0 & \left(1 - \frac{\eta_r + \eta_1}{2}\right)\beta & -d_3 - \lambda & 0 \\ 0 & \left(\frac{\eta_r + \eta_1}{2}\right)\beta & 0 & -d_3 - \lambda \end{vmatrix} = 0.$$

For the equilibrium point $E_1 = (\hat{T}, 0, 0, 0)$, (3.1) reduces to

$$\left(\lambda + \frac{2r}{T_{\max}} \sqrt{(r - d_1)^2 + \frac{4rs}{T_{\max}}}\right) (\lambda + d_3) [\lambda^2 + (d_2 + d_3)\lambda + d_2 d_3 (1 - R_0 e^{-\lambda\tau})] = 0.$$

Clearly, for $\tau = 0$, E_1 is locally asymptotically stable for $R_0 < 1$ and unstable for $R_0 > 1$. For $\tau > 0$, two eigenvalues are negative and the other two are given by

$$(3.2) \quad \lambda^2 + (d_2 + d_3)\lambda + d_2 d_3 (1 - R_0 e^{-\lambda\tau}) = 0.$$

Case I ($\tau > 0, R_0 > 1$): Let $F_1(\lambda) = \lambda^2 + (d_2 + d_3)\lambda$ and $F_2(\lambda) = d_2 d_3 (R_0 e^{-\lambda\tau} - 1)$, so that $F_1(\lambda) = F_2(\lambda)$. Clearly, $F_1(0) = 0$ and $F_1(\lambda) \rightarrow \infty$ as $\lambda \rightarrow \infty$; whereas $F_2(\lambda)$ is decreasing in λ . Furthermore, $F_2(0) = d_2 d_3 (R_0 - 1) > 0$ (since, $R_0 > 1$). Therefore, for some positive λ , the two functions $F_1(\lambda)$ and $F_2(\lambda)$ must intersect, implying the fact that the equation (3.2) has a positive root and we conclude that E_1 , the disease free steady state is unstable for positive delay and $R_0 > 1$.

Case II ($\tau > 0, R_0 < 1$): Our expectation in this case is (3.2) possesses negative roots and the disease free equilibrium is stable. Clearly, $\lambda^2 + (d_2 + d_3)\lambda = d_2 d_3 (R_0 e^{-\lambda\tau} - 1)$ does not possess a non-negative real root because $F_1(\lambda)$ is an increasing function for $\lambda \geq 0$, whereas $F_2(\lambda)$ is a decreasing function with $F_2(0) = R_0 - 1 < 0$. Therefore, we conclude that (3.2) will have roots with non-negative real parts if the roots are complex and should have been obtained from a pair of complex conjugate roots, which crosses the imaginary axis [8]. This implies that for some $\tau \geq 0$, (3.2) must have a pair of purely imaginary roots. Without any loss of generality, let $\lambda = i\omega$ ($\omega > 0$) be the root of (3.2). Substituting in (3.2) and separating the real and imaginary parts we get,

$$\begin{aligned} -\omega^2 + d_2 d_3 &= R_0 d_2 d_3 \cos(\omega\tau), \\ (d_2 + d_3)\omega &= R_0 d_2 d_3 \sin(\omega\tau). \end{aligned}$$

Eliminating the trigonometric function we get,

$$(3.3) \quad (\omega^2)^2 + (d_2^2 + d_3^2)\omega^2 + d_2^2 d_3^2 (1 - R_0^2) = 0.$$

Clearly, in (3.3), the sum of the roots are negative and the product of the roots are positive (as $R_0 < 1$) and consequently, (3.3) does not have any positive real roots, implying that there does not exist any ω for which $i\omega$ is a solution of (3.2). Following Rouché's theorem [13] (Theorem 9.17.4), we conclude that all the eigen values of the characteristic equation (3.2) have a negative real part for all $\tau \geq 0$. Therefore, E_1 is locally asymptotically stable for $R_0 < 1$.

3.2. Critical drug efficacy. The critical drug efficacy for this model is defined as (for details see [2])

$$\eta_c = 1 - \frac{2rd_2d_3}{\alpha\beta[(r-d_1)k + \sqrt{(r-d_1)^2k^2 + 4rsk}]} = 1 - \frac{T_0^*}{\widehat{T}}$$

where $T_0^* = \frac{d_2d_3}{\alpha\beta}$ is the number of uninfected hepatocytes in an infected person before treatment (obtained by putting $\eta_1 = \eta_r = 0$ in T^*) and \widehat{T} is the steady state of hepatocytes in an uninfected individual. η_c gives a measure for the threshold of the efficacies of drugs, interferon and ribavirin. If the combined efficacies exceed the critical value, HCV are eradicated whereas if $\eta < \eta_c$, HCV reaches a new steady state, lower than the previous steady state value [10, 2].

3.3. Hopf Bifurcation Analysis. For the equilibrium point $E_2 = (T^*, I^*, V_I^*, V_{NI}^*)$, (3.1) reduces to

$$(3.4) \quad (\lambda + d_3)[\lambda^3 + a_0\lambda^2 + a_1\lambda + a_2 + (b_1\lambda + b_2)e^{-\lambda\tau}] = 0$$

where,

$$\begin{aligned} a_0 &= d_2 + d_3 + \frac{s}{T^*} + \frac{rT^*}{T_{\max}}, \quad a_1 = d_2d_3 + (d_2 + d_3) \left(\frac{s}{T^*} + \frac{rT^*}{T_{\max}} \right), \\ a_2 &= d_2d_3 \left(\frac{s}{T^*} + \frac{rT^*}{T_{\max}} \right), \\ b_1 &= \frac{d_2rI^*}{T_{\max}} - (1 - c\eta_1) \left(1 - \frac{\eta_r + \eta_1}{2} \right) \alpha\beta T^* = \frac{d_2rI^*}{T_{\max}} - d_2d_3, \\ b_2 &= \frac{d_2d_3rI^*}{T_{\max}} + \left(d_2I^* - s - \frac{rT^{*2}}{T_{\max}} \right) (1 - c\eta_1) \left(1 - \frac{\eta_r + \eta_1}{2} \right) \alpha\beta \\ &= d_2d_3I^* \left(\frac{r}{T_{\max}} + \frac{d_2}{T^*} \right) - d_2d_3 \left(\frac{s}{T^*} + \frac{rT^*}{T_{\max}} \right). \end{aligned}$$

Clearly, the characteristic equation (3.4) has one negative eigenvalue, namely, $-d_3$ and we are left with

$$(3.5) \quad \lambda^3 + a_0\lambda^2 + a_1\lambda + a_2 + (b_1\lambda + b_2)e^{-\lambda\tau} = 0,$$

a transcendental equation (3.5) which has infinitely many eigenvalues and for which the classical Routh-Hurwitz condition for stability analysis fails.

In the absence of delay ($\tau = 0$), the characteristic equation (3.5) becomes

$$(3.6) \quad \lambda^3 + a_0\lambda^2 + (a_1 + b_1)\lambda + (a_2 + b_2) = 0,$$

By Routh-Hurwitz criteria, (3.6) will have negative real parts if $a_0 > 0$, $a_1 + b_1 > 0$, $a_2 + b_2 > 0$ and $(a_1 + b_1)a_0 - (a_2 + b_2) > 0$. Clearly, the first three conditions hold. Therefore, the equilibrium point E_2 is asymptotically stable in the absence of delay ($\tau = 0$), provided

$$(3.7) \quad \left[(d_2 + d_3) \left(\frac{s}{T^*} + \frac{rT^*}{T_{\max}} \right) + \frac{d_2rI^*}{T_{\max}} \right] \times \left(d_2 + d_3 + \frac{s}{T^*} + \frac{rT^*}{T_{\max}} \right) - d_2d_3I^* \left(\frac{r}{T_{\max}} + \frac{d_2}{T^*} \right) > 0$$

We now want to investigate the existence of purely imaginary roots of (3.5). Putting $\lambda = i\omega$ (ω is taken as positive) in the equation (3.5) and solving for real and imaginary parts, we have the system of transcendental equations as

$$(3.8) \quad a_0\omega^2 - a_2 = b_2 \cos(\omega\tau) + b_1\omega \sin(\omega\tau)$$

$$(3.9) \quad \omega^3 - a_1\omega = b_1\omega \cos(\omega\tau) - b_2 \sin(\omega\tau)$$

Squaring and adding (3.8) and (3.9), we obtain,

$$(3.10) \quad \omega^6 + A_1\omega^4 + A_2\omega^2 + A_3 = 0,$$

with

$$(3.11) \quad A_1 = (a_0^2 - 2a_1), \quad A_2 = (a_1^2 - b_1^2 - 2a_0a_2), \quad A_3 = a_2^2 - b_2^2.$$

The simplest assumption that (3.10) will have a positive root is $A_1 > 0$ and $A_3 < 0$. Clearly, $A_1 = d_2^2 + d_3^2 + \left(\frac{s}{T^*} + \frac{rT^*}{T_{\max}}\right)^2$ is positive. Therefore, for a positive root of the equation (3.10), we simply conclude that $a_2 - b_2 < 0$, that is,

$$2d_2d_3 \left(\frac{s}{T^*} + \frac{rT^*}{T_{\max}}\right) - d_2d_3I^* \left(\frac{r}{T_{\max}} + \frac{d_2}{T^*}\right) < 0$$

Therefore, we can say that there exists a unique positive root ω_0 satisfying (3.10), that is, the characteristic equation (3.4) will have purely imaginary roots of the form $\pm i\omega$. From (3.8) and (3.9), solving for $\cos(\omega\tau)$, we get

$$\cos(\omega\tau) = \frac{(a_0\omega^2 - a_2)b_2 + (\omega^3 - a_1\omega)b_1\omega}{b_2^2 + (b_1\omega)^2}.$$

Then τ_j corresponding to ω_0 is given by

$$(3.12) \quad \tau_j = \frac{1}{\omega_0} \arccos \left[\frac{(a_0\omega_0^2 - a_2)b_2 + (\omega_0^3 - a_1\omega_0)b_1\omega_0}{b_2^2 + (b_1\omega_0)^2} \right] + \frac{2j\pi}{\omega_0}, \quad j = 0, 1, 2, \dots$$

For $\tau = 0$, E_2 is locally asymptotically stable, provided (3.7) holds, therefore, by Butler's Lemma [19], E_2 remains locally asymptotically stable for $\tau < \tau_0$.

To establish the Hopf bifurcation at $\tau = \tau_0$, we have to show the transversality condition

$$\left[\frac{d(\operatorname{Re}\lambda)}{d\tau} \right]_{\tau = \tau_j} > 0.$$

Now, differentiating (3.5) with respect to τ , we get

$$[(3\lambda^2 + 2a_0\lambda + a_1) + e^{-\lambda\tau}b_1 - \tau e^{-\lambda\tau}(b_1\lambda + b_2)] \frac{d\lambda}{d\tau} = (b_1\lambda + b_2)e^{-\lambda\tau}\lambda.$$

This implies

$$\begin{aligned} \left[\frac{d\lambda}{d\tau} \right]^{-1} &= \frac{3\lambda^2 + 2a_0\lambda + a_1}{\lambda e^{-\lambda\tau}(b_1\lambda + b_2)} + \frac{b_1}{\lambda(b_1\lambda + b_2)} - \frac{\tau}{\lambda} \\ &= \frac{3\lambda^2 + 2a_0\lambda + a_1}{-\lambda(\lambda^3 + a_0\lambda^2 + a_1\lambda + a_2)} + \frac{b_1}{\lambda(b_1\lambda + b_2)} - \frac{\tau}{\lambda} \\ &= \frac{2\lambda^3 + a_0\lambda^2 - a_2}{-\lambda^2(\lambda^3 + a_0\lambda^2 + a_1\lambda + a_2)} + \frac{-b_2}{\lambda^2(b_1\lambda + b_2)} - \frac{\tau}{\lambda} \end{aligned}$$

Therefore,

$$\begin{aligned}
\Theta &= \text{sign} \left[\text{Re} \left(\frac{2\lambda^3 + a_0\lambda^2 - a_2}{-\lambda^2(\lambda^3 + a_0\lambda^2 + a_1\lambda + a_2)} + \frac{-b_2}{\lambda^2(b_1\lambda + b_2)} - \frac{\tau}{\lambda} \right) \right]_{\lambda = i\omega_0} \\
&= \frac{1}{\omega_0^2} \text{sign} \left[\text{Re} \left(\frac{(a_2 + a_0\omega_0^2) + i2\omega_0^3}{(a_0\omega_0^2 - a_2) + i(\omega_0^3 - a_1\omega_0)} + \frac{b_2}{b_2 + i(b_1\omega_0)} \right) \right] \\
&= \frac{1}{\omega_0^2} \text{sign} \left[\frac{(a_2 + a_0\omega_0^2)(a_0\omega_0^2 - a_2) + 2\omega_0^3(\omega_0^3 - a_1\omega_0)}{(a_0\omega_0^2 - a_2)^2 + (\omega_0^3 - a_1\omega_0)^2} + \frac{b_2^2}{b_2^2 + (b_1\omega_0)^2} \right] \\
&= \frac{1}{\omega_0^2} \text{sign} \left[\frac{2\omega_0^6 + (a_0^2 - 2a_1)\omega_0^4 + (b_2^2 - a_2^2)}{b_2^2 + (b_1\omega_0)^2} \right]
\end{aligned}$$

Clearly, $A_1 = a_0^2 - 2a_1$ is positive and by the assumption $A_3 = a_2^2 - b_2^2$ is negative, implying

$$\left[\frac{d(\text{Re}\lambda)}{d\tau} \right]_{\omega = \omega_0, \tau = \tau_j} > 0.$$

We summarize the preceding analysis in the form of a theorem.

THEOREM 3.1. *Suppose*

- (i) $R_0 > 1$.
 - (ii) $\left[(d_2 + d_3) \left(\frac{s}{T^*} + \frac{rT^*}{T_{\max}} \right) + \frac{d_2 r I^*}{T_{\max}} \right] \left(d_2 + d_3 + \frac{s}{T^*} + \frac{rT^*}{T_{\max}} \right) - d_2 d_3 I^* \left(\frac{r}{T_{\max}} + \frac{d_2}{T^*} \right) > 0$ is satisfied and
 - (iii) the largest positive simple root of (3.10) is ω_0 ,
- then E_2 , the endemic equilibrium point of the delay model is asymptotically stable when $\tau < \tau_0$ and unstable when $\tau > \tau_0$, where,

$$\tau_0 = \frac{1}{\omega_0} \arccos \left[\frac{(a_0\omega_0^2 - a_2)b_2 + (\omega_0^3 - a_1\omega_0)b_1\omega_0}{b_2^2 + (b_1\omega_0)^2} \right].$$

At τ passes through the critical point $\tau = \tau_0$, a family of periodic solutions bifurcates from E_2 , that is, a Hopf bifurcation occurs at $\tau = \tau_0$.

3.4. Estimation of the length of delay to preserve stability. It should be noted that the stability of bifurcating periodic orbits cannot be determined from the previous analysis, that is, in the neighborhood of τ_0 , existence of periodic solutions will depend on either for $\tau > \tau_0$ or for $\tau < \tau_0$. While investigating the stability of bifurcating periodic orbits, we now try to estimate the maximum length of delay to maintain the stability of the limit cycle. For this, we consider the space of real valued continuous functions, defined on $[-\tau, \infty)$, satisfying the initial conditions on $[-\tau, 0]$.

Let $T(t) = T^* + X(t)$, $I(t) = I^* + Y(t)$, $V_I(t) = V_I^* + Z(t)$, $V_{NI}(t) = V_{NI}^* + W(t)$. Linearizing the system (2.2) about the equilibrium point $E_2(T^*, I^*, V_I^*, V_{NI}^*)$, we get

$$\begin{aligned}
(3.13) \quad \frac{dX}{dt} &= \left(r - d_1 - \frac{2rT^*}{T_{\max}} - \frac{rI^*}{T_{\max}} - (1 - c\eta_1)\alpha V_I^* \right) X(t) - \frac{rT^*}{T_{\max}} Y(t) \\
&\quad - (1 - c\eta_1)\alpha T^* Z(t) \\
\frac{dY}{dt} &= (1 - c\eta_1)\alpha V_I^* X(t - \tau) - d_2 Y(t) + (1 - c\eta_1)\alpha T^* Z(t - \tau) \\
\frac{dZ}{dt} &= \left(1 - \frac{\eta_1 + \eta_r}{2} \right) \beta Y(t) - d_3 Z(t) \\
\frac{dW}{dt} &= \left(\frac{\eta_1 + \eta_r}{2} \right) \beta Y(t) - d_3 W(t).
\end{aligned}$$

Using Laplace transform of the linearized system (3.13), we obtain,

$$\begin{cases} \left(\delta - r + d_1 + \frac{2rT^*}{T_{\max}} + \frac{rI^*}{T_{\max}} + (1 - c\eta_1)\alpha V_I^* \right) L_X(\delta) = -\frac{rT^*}{T_{\max}} L_Y(\delta) \\ -(1 - c\eta_1)\alpha T^* L_Z(\delta) + X(0) \\ (\delta + d_2)L_Y(\delta) = (1 - c\eta_1)\alpha e^{-\delta\tau} V_I^* L_X(\delta) \\ +(1 - c\eta_1)\alpha e^{-\delta\tau} V_I^* K_1(\delta) + (1 - c\eta_1)\alpha e^{-\delta\tau} T^* L_Z(\delta) + (1 - c\eta_1)\alpha e^{-\delta\tau} T^* K_2(\delta) + Y(0) \\ (\delta + d_3)L_Z(\delta) = \left(1 - \frac{\eta_1 + \eta_r}{2}\right) \beta L_Y(\delta) + Z(0) \\ (\delta + d_3)L_W(\delta) = \left(\frac{\eta_1 + \eta_r}{2}\right) \beta L_Y(\delta) + W(0) \end{cases}$$

where, $K_1(\delta) = \int_{-\tau}^0 e^{-\delta t} X(t)dt$, $K_2(\delta) = \int_{-\tau}^0 e^{-\delta t} Z(t)dt$ and L_X, L_Y, L_Z and L_W are the Laplace transforms of $X(t), Y(t), Z(t)$ and $W(t)$ respectively.

Applying Nyquist criterion, we obtain the conditions for local asymptotic stability of $E_2(T^*, I^*, V_I^*, V_{NI}^*)$ as [19]

$$(3.14) \quad \text{Im}H(i\mu_0) > 0,$$

$$(3.15) \quad \text{Re}H(i\mu_0) = 0.$$

where $H(\delta) = (\delta^3 + a_0\delta^2 + a_1\delta + a_2) + e^{-\delta\tau}(b_1\delta + b_2)$, μ_0 being the smallest positive root of (3.15). It has already been proved that in the absence of delay, E_2 is locally asymptotically stable, provided (3.7) holds. Then, by virtue of Burlet's lemma [19], we can state that for sufficiently small $\tau > 0$, all the eigenvalues will continue to have negative real parts (by continuity), provided there is a guarantee that no eigenvalues with positive real parts bifurcates from infinity as τ increases from zero.

Inequality (3.14) and equation (3.15) gives

$$(3.16) \quad a_2 - a_0\mu_0^2 = -b_2 \cos(\mu_0\tau) - b_1\mu_0 \sin(\mu_0\tau)$$

$$(3.17) \quad -\mu_0^3 + a_1\mu_0 > b_2 \sin(\mu_0\tau) - b_1\mu_0 \cos(\mu_0\tau)$$

The sufficient conditions that guarantee that stability is obtained, if (3.16) and (3.17) are satisfied simultaneously, which we utilize to get an estimate of the length of the delay. Equation (3.16) gives

$$(3.18) \quad a_0\mu_0^2 = a_2 + b_2 \cos(\mu_0\tau) + b_1\mu_0 \sin(\mu_0\tau)$$

Taking the maximum value of $a_2 + b_2 \cos(\mu_0\tau) + b_1\mu_0 \sin(\mu_0\tau)$ subject to $|\sin(\mu_0\tau)| \leq 1, |\cos(\mu_0\tau)| \leq 1$, we get

$$(3.19) \quad \begin{aligned} a_0\mu_0^2 &\leq |a_2| + |b_2| + |b_1|\mu_0 \\ \Rightarrow a_0\mu_0^2 - |b_1|\mu_0 - (|a_2| + |b_2|) &= 0 \end{aligned}$$

So, if

$$\mu_+ = \frac{|b_1| + \sqrt{b_1^2 + 4a_0(|a_2| + |b_2|)}}{2a_0},$$

then from (3.19), we have $\mu_0 \leq \mu_+$.

From inequality (3.17), we get

$$(3.20) \quad \mu_0^2 \leq a_1 - \frac{b_2}{\mu_0} \sin(\mu_0\tau) + b_1 \cos(\mu_0\tau),$$

which continue to hold for sufficiently small $\tau > 0$. Substituting (3.18) in (3.20) and rearranging we get,

$$(3.21) \quad (b_2 - a_0 b_1)(\cos(\mu_0 \tau) - 1) + \left(b_1 \mu_0 + \frac{a_0 b_2}{\mu_0}\right) \sin(\mu_0 \tau) < a_0 a_1 - a_2 - b_2 - a_0 b_1$$

Using the bounds

$$(3.22) \quad (b_2 - a_0 b_1)(\cos(\mu_0 \tau) - 1) = 2(b_2 - a_0 b_1) \sin^2\left(\frac{\mu_0 \tau}{2}\right) \leq \frac{1}{2} |b_2 - a_0 b_1| \mu_+^2 \tau^2$$

and

$$(3.23) \quad \left(b_1 \mu_0 + \frac{a_0 b_2}{\mu_0}\right) \sin(\mu_0 \tau) \leq (b_1 \mu_+^2 + a_0 b_2) \tau$$

we obtain from (3.21), $N_1 \tau^2 + N_2 \tau < N_3$, where,

$$N_1 = \frac{1}{2} |b_2 - a_0 b_1| \mu_+^2, \quad N_2 = (b_1 \mu_+^2 + a_0 b_2), \quad N_3 = a_0 a_1 - a_2 - b_2 + a_0 b_1.$$

Thus, Nyquist criterion holds true for $0 \leq \tau \leq \tau_+$, where $\tau_+ = \frac{1}{2N_1} \left(-N_2 + \sqrt{N_2^2 + 4N_1 N_3}\right)$, which gives the maximum length of delay for maintaining the stability of the limit cycle.

3.5. Direction and stability of the Hopf bifurcation. In the subsection 3.3, we have obtained the condition for Hopf bifurcation at the critical value τ_j and succeeded to obtain explicitly the expression for τ_j by using the normal form and manifold theory and following the ideas of Hassard et al. [23]. In the coming analysis, our initial assumption is that the system (2.2) exhibits Hopf bifurcation, which in turn implies that $\pm i\omega$ are the corresponding purely imaginary roots of the characteristic equation at the infected equilibrium point $E_2(T^*, I^*, V_I^*, V_{NI}^*)$.

Using the transformation $u_1(t) = T(t) - T^*$, $u_2(t) = I(t) - I^*$, $u_3(t) = V_I(t) - V_I^*$, $u_4(t) = V_{NI}(t) - V_{NI}^*$, $x_i(t) = u_i(\tau t)$, ($i = 1, 2, 3, 4$), $\tau = \tau_j + \mu$, the system (2.2) is converted to a functional differential equation (FDE) in $C = C([-1, 0], R^4)$

$$(3.24) \quad \frac{dx}{dt} = L_\mu(x_t) + f(\mu, x_t),$$

where $(x_1(t), x_2(t), x_3(t), x_4(t))^T \in R^4$ and the mapping $L_\mu : C \rightarrow R$, $f : R \times C \rightarrow R$, are respectively given by

$$L_\mu(\phi) = (\tau_j + \mu) \begin{pmatrix} r - d_1 - \frac{2rT^*}{T_{max}} - \frac{rI^*}{T_{max}} - (1 - c\eta_1)\alpha V_I^* & -\frac{rT^*}{T_{max}} & -(1 - c\eta_1)\alpha T^* & 0 \\ 0 & -d_2 & 0 & 0 \\ 0 & \left(1 - \frac{\eta_r + \eta_1}{2}\right)\beta & -d_3 & 0 \\ 0 & \left(\frac{\eta_r + \eta_1}{2}\right)\beta & 0 & -d_3 \end{pmatrix} \begin{pmatrix} \phi_1(0) \\ \phi_2(0) \\ \phi_3(0) \\ \phi_4(0) \end{pmatrix} \\ + (\tau_j + \mu) \begin{pmatrix} 0 & 0 & 0 & 0 \\ (1 - c\eta_1)\alpha V_I^* & 0 & (1 - c\eta_1)\alpha T^* & 0 \\ 0 & 0 & 0 & 0 \\ 0 & 0 & 0 & 0 \end{pmatrix} \begin{pmatrix} \phi_1(-1) \\ \phi_2(-1) \\ \phi_3(-1) \\ \phi_4(-1) \end{pmatrix}$$

and

$$f(\mu, \phi) = (\tau_j + \mu) \begin{pmatrix} -\frac{r}{T_{max}} \phi_1^2(0) - \frac{r}{T_{max}} \phi_1(0) \phi_2(0) - (1 - c\eta_1)\alpha \phi_1(0) \phi_3(0) \\ (1 - c\eta_1)\alpha \phi_1(-1) \phi_3(-1) \\ 0 \\ 0 \end{pmatrix}$$

By virtue of Riesz representation theorem, we can find a function $\eta(\theta, \mu)$ of bounded variation for $\theta \in [-1, 0]$, such that

$$(3.25) \quad L_\mu(\phi) = \int_{-1}^0 \phi(\theta) d\eta(\theta, 0)$$

for $\phi \in C$. We choose

$$(3.26) \quad \eta(\theta, \mu) = (\tau_j + \mu) \begin{pmatrix} F & -\frac{rT^*}{T_{max}} & -(1 - c\eta_1)\alpha T^* & 0 \\ 0 & -d_2 & 0 & 0 \\ 0 & (1 - \frac{\eta_r + \eta_1}{2})\beta & -d_3 & 0 \\ 0 & (\frac{\eta_r + \eta_1}{2})\beta & 0 & -d_3 \end{pmatrix} \delta(\theta) \\ - (\tau_j + \mu) \begin{pmatrix} 0 & 0 & 0 & 0 \\ (1 - c\eta_1)\alpha V_I^* & 0 & (1 - c\eta_1)\alpha T^* & 0 \\ 0 & 0 & 0 & 0 \\ 0 & 0 & 0 & 0 \end{pmatrix} \delta(\theta + 1),$$

where δ is the Dirac delta function. Let

$$A(\mu)\phi = \begin{cases} \frac{d\phi(\theta)}{d\theta}, & \theta \in [-1, 0), \\ \int_{-1}^0 d\eta(\mu, s_1)\phi(s_1), & \theta = 0, \end{cases}$$

and

$$R(\mu)\phi = \begin{cases} 0, & \theta \in [-1, 0), \\ f(\mu, \phi), & \theta = 0, \end{cases}$$

for $\phi \in C^1([-1, 0], R^4)$, then system (3.24) is equivalent to

$$(3.27) \quad \dot{x}_t = A(\mu)x_t + R(\mu)x_t,$$

where $x_t(\theta) = x(t + \theta)$ for $\theta \in [-1, 0]$. Again let

$$A^*\psi(s_1) = \begin{cases} -\frac{d\psi(s_1)}{ds_1}, & s_1 \in (-1, 0], \\ \int_{-1}^0 d\eta^T(t, 0)\psi(-t), & s_1 = 0, \end{cases}$$

for $\psi \in C^1([-1, 0], (R^4)^*)$. We define a bilinear inner product

$$(3.28) \quad \langle \psi(s_1), \phi(\theta) \rangle = \bar{\psi}(0)\phi(0) - \int_{-1}^0 \int_{\xi=0}^\theta \bar{\psi}(\xi - \theta) d\eta(\theta)\phi(\xi) d\xi, \quad [\eta(\theta) = \eta(\theta, 0)]$$

$A(0)$ and A^* are called as adjoint operators. It can be easily shown that $\pm i\omega_0\tau_j$ are eigenvalues of $A(0)$. Therefore, $\pm i\omega_0\tau_j$ are also eigenvalues of A^* .

Let $q(\theta) = (1, a, b, c_1)^T e^{i\omega_0\tau_j\theta}$ be the eigenvector of $A(0)$ corresponding to $i\omega_0\tau_j$, then $A(0)q(\theta) = i\omega_0\tau_j q(\theta)$. Using (3.25), (3.25), (3.26) and the definition of $A(0)$, we obtain,

$$\tau_j \begin{pmatrix} i\omega_0 - F & \frac{rT^*}{T_{max}} & (1 - c\eta_1)\alpha T^* & 0 \\ -(1 - c\eta_1)\alpha V_I^* e^{-i\omega_0\tau_j} & i\omega_0 + d_2 & -(1 - c\eta_1)\alpha T^* e^{-i\omega_0\tau_j} & 0 \\ 0 & -\left(1 - \frac{\eta_r + \eta_1}{2}\right)\beta & i\omega_0 + d_3 & 0 \\ 0 & -\left(\frac{\eta_r + \eta_1}{2}\right)\beta & 0 & i\omega_0 + d_3 \end{pmatrix} q(0) = \begin{pmatrix} 0 \\ 0 \\ 0 \\ 0 \end{pmatrix}$$

We can easily obtain $q(0) = (1, a, b, c_1)^T$, where

$$a = \frac{(\mathrm{i}\omega_0 + d_3)(1 - c\eta_1)\alpha V_I^* e^{-\mathrm{i}\omega_0\tau_j}}{(\mathrm{i}\omega_0 + d_2)(\mathrm{i}\omega_0 + d_3) - (1 - c\eta_1)\left(1 - \frac{\eta_r + \eta_1}{2}\right)\alpha\beta T^* e^{-\mathrm{i}\omega_0\tau_j}}, \quad b = \frac{\left(1 - \frac{\eta_r + \eta_1}{2}\right)\beta a}{(\mathrm{i}\omega_0 + d_3)}, \quad c_1 = \frac{\left(\frac{\eta_r + \eta_1}{2}\right)\beta a}{(\mathrm{i}\omega_0 + d_3)}.$$

Again, let $q^*(s_1) = D(1, a^*, b^*, c_1^*)e^{\mathrm{i}\omega_0\tau_j s_1}$ be the eigenvector of A^* corresponding to $-\mathrm{i}\omega_0\tau_j$. In the similar manner we obtain,

$$a^* = \frac{-(\mathrm{i}\omega_0 + F)}{(1 - c\eta_1)\alpha V_I^* e^{-\mathrm{i}\omega_0\tau_j}}, \quad b^* = \frac{\frac{rT^*}{T_{max}} + (-\mathrm{i}\omega_0 + d_2)a^*}{\left(1 - \frac{\eta_r + \eta_1}{2}\right)\beta}, \quad c_1^* = 0.$$

To assure $\langle q^*, q(\theta) \rangle = 1$, we use (3.28) to calculate D as follows:

$$\begin{aligned} \langle q^*, q(\theta) \rangle &= \overline{D}(1, \overline{a^*}, \overline{b^*}, \overline{c_1^*})(1, a, b, c_1)^T - \int_{-1}^0 \int_{\xi=0}^{\theta} \overline{D}(1, \overline{a^*}, \overline{b^*}, \overline{c_1^*})e^{-\mathrm{i}\omega_0\tau_j(\xi-\theta)} d\eta(\theta)(1, a, b, c_1)^T e^{\mathrm{i}\omega_0\tau_j\xi} d\xi \\ &= \overline{D} \left\{ 1 + a\overline{a^*} + b\overline{b^*} - \int_{-1}^0 (1, \overline{a^*}, \overline{b^*}, 0)\theta e^{\mathrm{i}\omega_0\tau_j\theta} d\eta(\theta)(1, a, b, c_1)^T \right\} \\ &= \overline{D} \{ 1 + a\overline{a^*} + b\overline{b^*} + \tau_j e^{-\mathrm{i}\omega_0\tau_j} (1 - c\eta_1)\alpha\overline{a^*}(V_I^* + bT^*) \} \end{aligned}$$

Choosing

$$D = \frac{1}{1 + \overline{a}a^* + \overline{b}b^* + \tau_j e^{\mathrm{i}\omega_0\tau_j} (1 - c\eta_1)\alpha a^*(V_I^* + bT^*)},$$

we achieve the property $\langle q^*, q(\theta) \rangle = 1$.

To compute the coordinates describing the center manifold \mathbf{C}_0 at $\mu = 0$, we apply the idea of Hassard et al. [23]. Denoting x_t to be the solution of (3.27) at $\mu = 0$, we define

$$(3.29) \quad z(t) = \langle q^*, x_t \rangle, \quad W(t, \theta) = x_t(\theta) - 2\mathrm{Re}\{z(t)q(\theta)\}$$

On center manifold \mathbf{C}_0 , we have

$$W(t, \theta) = W(z(t), \overline{z}(t), \theta),$$

where

$$(3.30) \quad W(z, \overline{z}, \theta) = W_{20}(\theta)\frac{z^2}{2} + W_{11}(\theta)z\overline{z} + W_{02}(\theta)\frac{\overline{z}^2}{2} + W_{30}(\theta)\frac{z^3}{6} + \dots,$$

z and \overline{z} are local coordinates for center manifold \mathbf{C}_0 in the direction of q^* and $\overline{q^*}$. The expression $W(z, \overline{z}, \theta)$ will be real provided x_t is real and we are interested in real solutions only. For solution $x_t \in \mathbf{C}_0$ of (3.27), since $\mu = 0$, we have

$$\dot{z}(t) = \mathrm{i}\omega_0\tau_j z + \overline{q^*}(0)f(0, W(z, \overline{z}, 0) + 2\mathrm{Re}\{zq(\theta)\}) \doteq \mathrm{i}\omega_0\tau_j z + \overline{q^*}(0)f_0(z, \overline{z}).$$

which is rewritten as

$$\dot{z}(t) = \mathrm{i}\omega_0\tau_j z(t) + g(z, \overline{z}),$$

where

$$(3.31) \quad g(z, \overline{z}) = \overline{q^*}(0)f_0(z, \overline{z}) = g_{20}\frac{z^2}{2} + g_{11}z\overline{z} + g_{02}\frac{\overline{z}^2}{2} + g_{21}\frac{z^2\overline{z}}{2} + \dots$$

Then (3.29) and (3.30) gives

$$\begin{aligned} x_t(\theta) &= W(t, \theta) + 2\text{Re}\{z(t)q(t)\} \\ &= W_{20}(\theta)\frac{z^2}{2} + W_{11}(\theta)z\bar{z} + W_{02}(\theta)\frac{\bar{z}^2}{2} + (1, a, b, c_1)^T e^{i\omega_0\tau_j\theta} z \\ &\quad + (1, \bar{a}, \bar{b}, \bar{c}_1)^T e^{-i\omega_0\tau_j\theta} \bar{z} + \dots, \end{aligned}$$

From the definition of $g(z, \bar{z})$ we have

$$\begin{aligned} g(z, \bar{z}) &= \bar{q}^*(0)f_0(z, \bar{z}) = \bar{q}^*(0)f(0, x_t) \\ &= \tau_j \bar{D}(1, \bar{a}^*, \bar{b}^*, 0) \begin{pmatrix} -\frac{r}{T_{max}}x_{1t}^2(0) - \frac{r}{T_{max}}x_{1t}(0)x_{2t}(0) - (1 - c\eta_1)\alpha x_{1t}(0)x_{3t}(0) \\ (1 - c\eta_1)\alpha x_{1t}(-1)x_{3t}(-1) \\ 0 \\ 0 \end{pmatrix} \\ &= -\tau_j \bar{D} \left\{ \frac{r}{T_{max}} \left[z + \bar{z} + W_{20}^{(1)}(0)\frac{z^2}{2} + W_{11}^{(1)}(0)z\bar{z} + W_{02}^{(1)}(0)\frac{\bar{z}^2}{2} + o(|(z, \bar{z})|^3) \right]^2 \right. \\ &\quad + \frac{r}{T_{max}} \left[z + \bar{z} + W_{20}^{(1)}(0)\frac{z^2}{2} + W_{11}^{(1)}(0)z\bar{z} + W_{02}^{(1)}(0)\frac{\bar{z}^2}{2} + o(|(z, \bar{z})|^3) \right] \\ &\quad (3.32) \quad \times \left[az + \bar{a}\bar{z} + W_{20}^{(2)}(0)\frac{z^2}{2} + W_{11}^{(2)}(0)z\bar{z} + W_{02}^{(2)}(0)\frac{\bar{z}^2}{2} + o(|(z, \bar{z})|^3) \right] \\ &\quad + \alpha_1 \left[be^{-i\omega_0\tau_j}z + \bar{b}e^{i\omega_0\tau_j}\bar{z} + W_{20}^{(3)}(-1)\frac{z^2}{2} + W_{11}^{(3)}(-1)z\bar{z} + W_{02}^{(3)}(-1)\frac{\bar{z}^2}{2} + o(|(z, \bar{z})|^3) \right] \\ &\quad \times \left[e^{-i\omega_0\tau_j}z + e^{i\omega_0\tau_j}\bar{z} + W_{20}^{(1)}(-1)\frac{z^2}{2} + W_{11}^{(1)}(-1)z\bar{z} + W_{02}^{(1)}(-1)\frac{\bar{z}^2}{2} + o(|(z, \bar{z})|^3) \right] \Big\} \\ &\quad + \gamma \left[be^{-i\omega_0\tau_j}z + \bar{b}e^{i\omega_0\tau_j}\bar{z} + W_{20}^{(3)}(-1)\frac{z^2}{2} + W_{11}^{(3)}(-1)z\bar{z} + W_{02}^{(3)}(-1)\frac{\bar{z}^2}{2} + o(|(z, \bar{z})|^3) \right] \\ &\quad \times \left[e^{-i\omega_0\tau_j}z + e^{i\omega_0\tau_j}\bar{z} + W_{20}^{(1)}(-1)\frac{z^2}{2} + W_{11}^{(1)}(-1)z\bar{z} + W_{02}^{(1)}(-1)\frac{\bar{z}^2}{2} + o(|(z, \bar{z})|^3) \right] \end{aligned}$$

Comparing the coefficients with (3.31), we get,

$$\begin{aligned} g_{20} &= -2\tau_j \bar{D} \left[(1 + a)\frac{r}{T_{max}} + (1 - c\eta_1)\alpha be^{-2i\omega_0\tau_j} - (1 - c\eta_1)\alpha \bar{b}\bar{a}^* e^{-2i\omega_0\tau_j} \right] \\ g_{11} &= -2\tau_j \bar{D} \left[(1 + \text{Re}(a))\frac{r}{T_{max}} + (1 - c\eta_1)\alpha \text{Re}(b) - (1 - c\eta_1)\alpha \text{Re}(b)\bar{a}^* \right] \\ g_{02} &= -2\tau_j \bar{D} \left[(1 + \bar{a})\frac{r}{T_{max}} + (1 - c\eta_1)\alpha \bar{b}e^{2i\omega_0\tau_j} - (1 - c\eta_1)\alpha \bar{b}\bar{a}^* e^{2i\omega_0\tau_j} \right] \\ g_{21} &= -2\tau_j \bar{D} \left[2\frac{r}{T_{max}}W_{11}^{(1)}(0) + \frac{r}{T_{max}}W_{20}^{(1)}(0) + \frac{r}{T_{max}}\{aW_{11}^{(1)}(0) + \frac{1}{2}\bar{a}W_{20}^{(1)}(0) \right. \\ &\quad + \frac{1}{2}W_{20}^{(2)}(0) + W_{11}^{(2)}(0)\} + (1 - c\eta_1)\alpha\{W_{11}^{(3)}(-1)e^{-i\omega_0\tau_j} + \frac{1}{2}W_{20}^{(3)}(-1)e^{i\omega_0\tau_j} \\ &\quad + \frac{1}{2}\bar{b}W_{20}^{(1)}(-1)e^{i\omega_0\tau_j} + bW_{11}^{(1)}(-1)e^{-i\omega_0\tau_j}\} - (1 - c\eta_1)\alpha\bar{a}^*\{W_{11}^{(3)}(-1)e^{-i\omega_0\tau_j} \\ &\quad + \frac{1}{2}W_{20}^{(3)}(-1)e^{i\omega_0\tau_j} + \frac{1}{2}\bar{b}W_{20}^{(1)}(-1)e^{i\omega_0\tau_j} + bW_{11}^{(1)}(-1)e^{-i\omega_0\tau_j}\} \Big] \end{aligned}$$

Since $W_{20}(\theta)$ and $W_{11}(\theta)$ are in the expression of g_{21} , we need to compute them. The calculation is shown in the Appendix. Furthermore, g_{21} can be expressed using the parameters and the delay in the system. Therefore, we can compute

$$\begin{aligned}
 c_{11}(0) &= \frac{i}{2\omega_0\tau_j} \left(g_{20}g_{11} - 2|g_{11}|^2 - \frac{|g_{02}|^2}{3} \right) + \frac{g_{21}}{2}, \\
 \mu_2 &= -\frac{\operatorname{Re}\{c_{11}(0)\}}{\operatorname{Re}\{\lambda'(\tau_j)\}}, \\
 \beta_2 &= 2\operatorname{Re}(c_{11}(0)) \quad \text{and} \\
 T_2 &= -\frac{\operatorname{Im}\{c_{11}(0)\} + \mu_2\operatorname{Im}\{\lambda'(\tau_j)\}}{\omega_0\tau_j}.
 \end{aligned}
 \tag{3.33}$$

The expressions in (3.33) gives the quantification of the bifurcating periodic solutions in the center manifold at the critical value (τ_0) of the time lag. The direction of the Hopf bifurcation is determined from the sign of μ_2 . The Hopf bifurcation is forward or backward according as $\mu_2 > 0$ or $\mu_2 < 0$ and the bifurcating periodic solution exists for $\tau > \tau_0$ and $\tau < \tau_0$ respectively. The sign of β_2 quantifies the stability of the bifurcating periodic solution; for $\beta_2 < 0$, the solution is stable and unstable if $\beta_2 > 0$. Finally, T_2 determines the period of the bifurcating periodic solution. The period is increasing if $T_2 > 0$ and decreasing if $T_2 < 0$.

4. Numerical results and its biological implications. We now simulate the system (2.2) to observe the effect of intracellular delay on the dynamics of hepatitis C virus with therapy. We verify our model with two sets of parameter obtained from [10] (see table 1 and 2), starting with parameter set 1. We have taken the viral replication time (τ) in the range of 24 hours to 36 hours [16, 22]. Throughout the discussion, we have considered η as the combined drug efficacy, given by

$$1 - \eta = (1 - c\eta_1) \left(1 - \frac{\eta_r + \eta_1}{2} \right),$$

along with η_c , the critical drug efficacy. Our discussion will revolve around R_0 , the basic reproduction number and its relation with the critical drug efficacy η_c . Please note, the initial viral load for numerical simulation is 10^7 copies/ml, which is around the endemic equilibrium point and hence

$$\begin{aligned}
 R_0 > 1 \quad \Rightarrow \quad \frac{\hat{T}}{T^*} > 1 \quad \Rightarrow \quad \hat{T} \frac{\alpha\beta(1-\eta)}{d_2d_3} > 1 \\
 \Rightarrow \quad \eta < 1 - \frac{d_2d_3}{\alpha\beta\hat{T}} = \eta_c
 \end{aligned}
 \tag{4.1}$$

This implies when $\eta < \eta_c$, $R_0 > 1$ and the viral load reaches the endemic equilibrium point. But, when $\eta > \eta_c$, $R_0 < 1$, the endemic equilibrium point becomes negative and exchanges stability with the uninfected steady state and disease free equilibrium point is achieved.

Table 1

Parameter	Parameter values	Units
s	1.0	cells day ⁻¹ ml ⁻¹ [10]
r	2.0	day ⁻¹ [10]
T_{\max}	3.6×10^7	cells ml ⁻¹ [10]
α	2.25×10^{-7}	ml virions ⁻¹ day ⁻¹ [10]
β	2.9	virions day ⁻¹ [10]
d_1	0.01	day ⁻¹ [10]
d_2	1.0	day ⁻¹ [10]
d_3	6.0	day ⁻¹ [10]

Table 2

Parameter	Parameter values	Units
s	3.7×10^4	cells day ⁻¹ ml ⁻¹ [10]
r	0.73	day ⁻¹ [10]
T_{\max}	0.6×10^7	cells ml ⁻¹ [10]
α	1.8×10^{-7}	ml virions ⁻¹ day ⁻¹ [10]
β	13.9	virions day ⁻¹ [10]
d_1	2.4×10^{-3}	day ⁻¹ [10]
d_2	0.06	day ⁻¹ [10]
d_3	13.9	day ⁻¹ [10]

Effect of interferon monotherapy: We first consider interferon, a mixture of proteins, having antiviral and immunomodulating effects, to illustrates interferon monotherapy on viral dynamics in the presence of intracellular delay. Hepatitis C virus declines as well as the dynamics of infected and uninfected hepatocytes are shown in figure 4.1.

The viral decline is biphasic in nature, mimicking the kinetics of the viral decline in patients responding to interferon monotherapy. From the figure we conclude that the first phase decline occurs for about (48-52) hours, following by a slow second phase decline starting at 52 hours. This behavior has been observed clinically [25, 34]. The wavy nature of the second phase decline is due to the effect of intracellular delay. As the viral load declines, the infected hepatocytes also decline and the number of uninfected hepatoocytes reaches large steady state value. However, the standard interferon regime sometimes fails to control HCV, which are the case of non-responders. This dynamics has been portrayed in figure 4.2, where there is a first phase decline followed by a flat phase, that is, the viral load approaches an endemic steady state. The infectious hepatocytes and noninfectious viruses also exhibit the same behavior. Please note, though the interferon efficacy is high ($\eta_1 = 0.80$), the combined efficacy $\eta = 0.64 < \eta_c (= 0.745)$. Since, $\eta < \eta_c$ implies $R_0 > 1$, the viral load showing minor decline will never converge to E_0 and ultimately converge to a new steady state. This means that in non-responders, the efficacies due to interferon fail to reach the critical drug efficacy, and this has been confirmed clinically too [4, 3].

Effect of ribavirin monotherapy: Ribavirin monotherapy has not been effective for the treatment of hepatitis C viral infection and our model also certifies that. The effect of ribavirin monotherapy on HCV is shown in figure 4.3, where ribavirin fails to clear the viral load. Even though the efficacy of ribavirin is 0.98 (figure 4.3),

its combined efficacy as calculated by is 0.68, which is less than $\eta_c (= 0.745)$, implying $R_0 > 1$. Several experiments have been conducted [12, 11, 5] to evaluate the effect of ribavirin for the treatment of hepatitis C virus but no virologic end of treatment response (ETR) were observed in all these experiments. In most of these cases, HCV RNA level remains constant after 3-6 months of ribavirin monotherapy compared within pretreatment values [12, 11].

Effect of combined therapy: To achieve the goal of minimizing the viral load of HCV, current standard treatment consists of the combination of pegylated interferon and ribavirin [26]. Thus, we conclude that when interferon efficacy is small, ribavirin enhances treatment level by turning progeny virions non-infections, resulting in a second phase decline and the patient attains SVR, that is, the concentration of the virus in the patient's blood falls below the detection limit (100 copies/ml) during the combined therapy (figure 4.4). Experimental observation also confirm this fact [24, 26, 31]. The combined therapy of pegylated interferon and ribavirin also results in triphasic decline of viral load in some patients [24]. Figure 4.5 shows triphasic decline where the first phase shows a sharp drop in the viral load followed by a shoulder second phase (flat phase) after which the viral load decline continues in oscillations (third phase decline) and the patient attains SVR in approximately 25 days.

Figure 4.6 shows that the dynamics of our model are in agreement with the behavioral pattern of HCV in 12 patients obtained from the study, conducted at the University of Sao Paulo Hospital das clinicas and was approved by the ethics in research committee [9]. The patients were treated with pegylated interferon and ribavirin for 48 weeks and their detailed analysis were recorded (denoted by * in the figure). Figure A, B, C, D, E, F, G, H, I show the behavior of HCV RNA levels during the first 12-14 weeks of PEG-IFN- α -2a monotherapy. The graph obtained from the model (continuous line) matches with the patient data (*) [9]. Figure J is the case of non-responders and figures K and L are the case of non-SVR.

We next consider the second set of parameters given in the table 2, for verification of the model (2.2). With these set of parameters, theorem 3.1 holds. It is observed that without delay there exist a unique interior equilibrium point E_2 , which is locally asymptotically stable. Using the same set of parameters, we obtain, we $A_1 > 0$ and $A_3 < 0$, which indicates the existence of a positive root. We also calculate $w_0 = 0.07321$ by solving (3.10). Following theorem 1 in [7], we can say that stability switch may occur as the value of τ increases. In this case stability switch occurs at $\tau_0 = 24.1$ hours (calculated from (3.12) by putting $j = 0$), where the dynamics of the system changes from a stable steady state to stable oscillatory state. The calculated value of τ_0 also certifies our analytical estimation of the length of delay to preserve stability. Therefore, by Butler's lemma, E_2 remains stable for $\tau < \tau_0 (= 24.1 \text{ hours})$. For $\tau = 24.1$ hours Hopf bifurcation occurs resulting in stable periodic solution and at the bifurcated point, a stable limit cycle is formed (figure 4.7). We observe a stability switch as τ crosses the threshold ($\tau = 24.1$) hours and shows aperiodic solutions. Please note that we have not provided figures for $\tau < \tau_0$ and $\tau > \tau_0$ as these values of τ_0 are unrealistic as far as the patient's data are concerned.

5. Summary and Discussions. Several studies have used mathematical models to provide insights into the mechanism and dynamics of the progression of hepatitis C viral infection. It is of both mathematical and biological interest to determine the

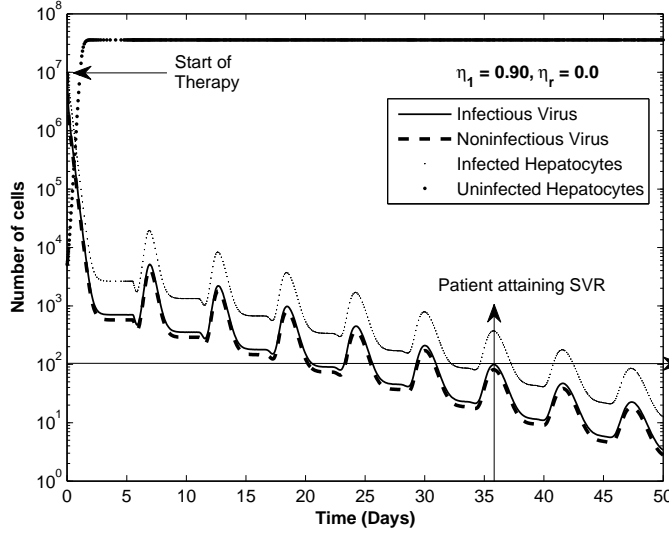


FIG. 4.1. Interferon monotherapy in presence of intracellular delay ($\tau = 22.0$ hours), where the parameter set is taken from Table 1. with initial conditions $(10^7, 10^7, 10^7, 10^7)$. The dynamics of all the state variables is shown in the figure. The hepatitis C viral load declines, which is biphasic in nature. From the start of the therapy, the first phase of virus decline occurs for (48-52) hours followed by a slow second phase till the patient reaches SVR in 36 days (shown by intersection of arrows). The infected hepatocytes and non-infectious virus also follow the same pattern of decline. The wavy nature of the decline is due to the presence of intracellular delay. The uninfected hepatocytes reaches a high steady state value ranging between $(10^7 - 10^8)$ cells, which has been observed in healthy patients. Please note that the uninfected hepatocytes though starts with the initial value of 10^7 cells, sharply declines when the viral load is high initially and regains its normal range once SVR has been achieved.

cause of sustained oscillation, which can be the result of intracellular delay. The main goal of this paper is to investigate how the delay affects the overall disease progression and mathematically, how the dynamics of the system is affected by the delay.

We have studied a modified HCV model with four state variables, namely, target cells, infected hepatocytes, infected and non-infected virions, along with an intracellular delay and combined drug therapy (interferon and ribavirin). The basic reproduction number of the hepatitis C virus has been used largely in understanding the dynamics of the viral infection. The influence of time delay on the stability of the equilibrium states has been discussed. We have proved that the local stability of the disease free steady state is independent of the delay. However, for the endemic equilibrium state, an increase in delay can destabilize the system, leading to hopf bifurcation and periodic solutions. The estimation of the length of delay to preserve stability has been obtained. Also, the direction and stability of the Hopf bifurcation have been studied.

The numerical study of the system focused on two aspects, namely, the dynamics of the system on two different parameter sets and validation of the model with the virus behavioral pattern of 12 patients, under the influence of interferon monotherapy and combined therapy with ribavirin. Our results mimic the behavior of HCV in

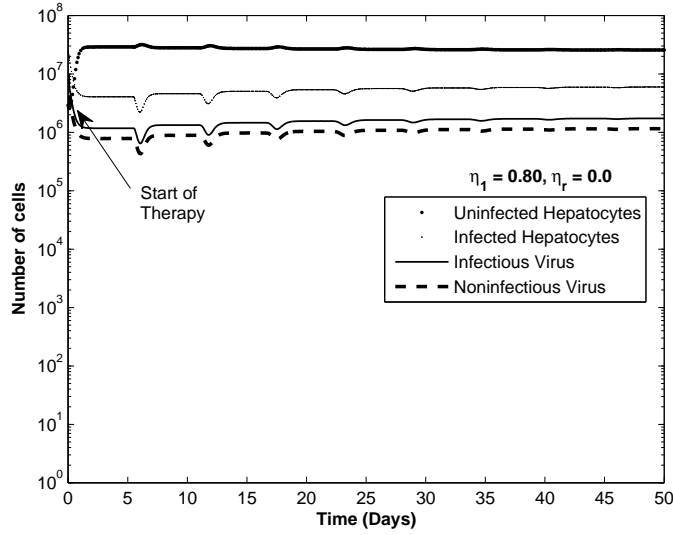


FIG. 4.2. Non-responders in the case of Interferon monotherapy in presence of intracellular delay ($\tau = 22.0$ hours), where the parameter set is taken from Table 1. with initial conditions $(10^7, 10^7, 10^7, 10^7)$. There is a short first phase decline, followed by a flat phase, where the hepatitis C virus ceases to decline and reaches the endemic steady state. This means that the drug interferon fails to reach the critical drug efficacy, so needed to eradicate hepatitis C virus and achieve SVR.

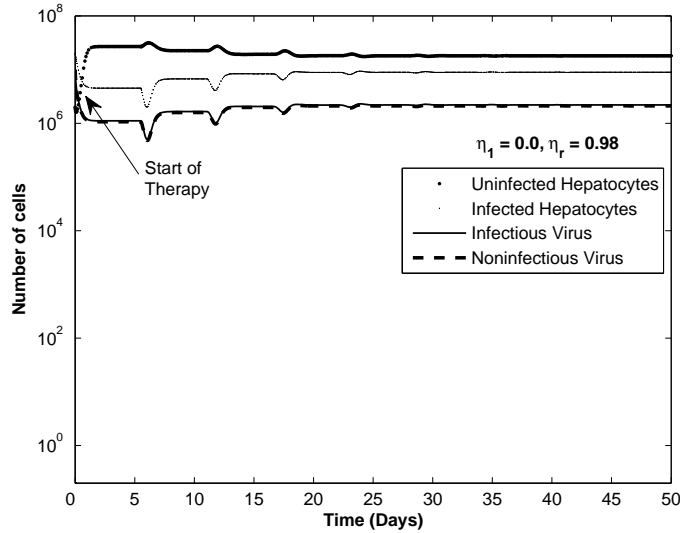


FIG. 4.3. Ribavirin monotherapy in presence of intracellular delay ($\tau = 22.0$ hours), where the parameter set is taken from Table 1. with initial conditions $(10^7, 10^7, 10^7, 10^7)$. The dynamics of all the state variables is shown in the figure, where ribavirin fails to clear the viral load and hepatitis C virus remains more or less constant during the therapy.

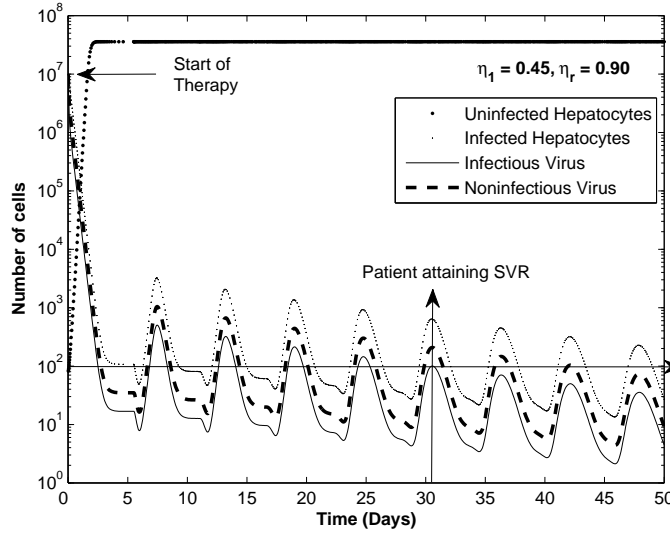


FIG. 4.4. Dynamics of hepatitis C virus during combined therapy in presence of intracellular delay ($\tau = 22.0$ hours), where the parameter set is taken from Table 1 with initial conditions $(10^7, 10^7, 10^7, 10^7)$. From the figure it is observed that when interferon efficacy is small, ribavirin enhances treatment level by turning infectious virus to non-infectious and the concentration of virus in the patient's blood falls below the detection limit of 100 copies/ml. The pattern of decline is wavy due to the delay effect and the patient attains SVR in 31 days (shown by intersection of arrows), which is a little faster than interferon monotherapy.

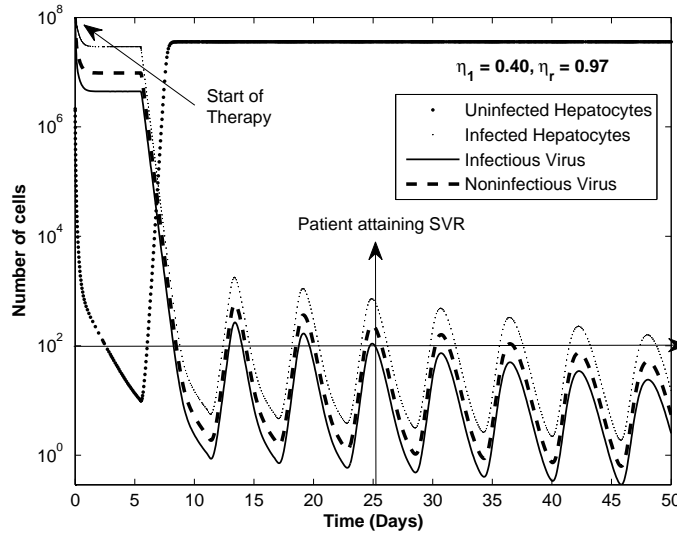


FIG. 4.5. Triphasic decline in hepatitis C viral dynamics in presence of intracellular delay ($\tau = 22.0$ hours), where the parameter set is taken from Table 1 with initial conditions $(10^7, 10^7, 10^7, 10^7)$. The first phase decline occurs for (24-36) hours followed by a shoulder (flat) phase, which continues for (1.5-5) days. Thus, there is a third phase decline, which happens in oscillation due to the presence of delay and SVR is achieved in 25 days.

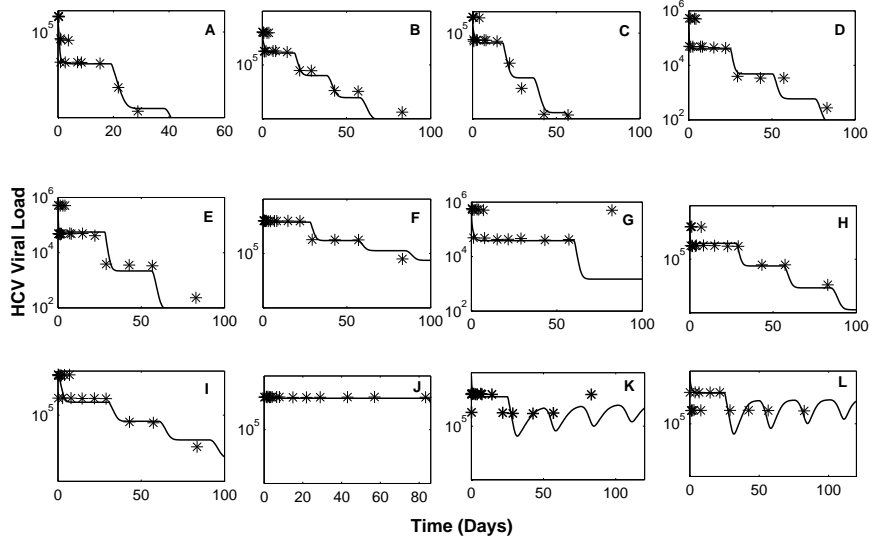


FIG. 4.6. Model validation with data obtained from 12 patients who were undergoing treatment with PEG-IFN- α -2a serum concentration at the University of Sao Paulo hospital das clinicas. The hepatitis C virus behavioral data of the patients which are shown in * are obtained from [9], page 464, figure2. In this figure, A-I are the responses of the model with interferon monotherapy (continuous line) which matches with the data (*). J is non-responder, K and L are non-SVR. All the parameter values are taken from Table 1, with $\tau_{au} = 22$ hours.

patients observed clinically with the first set of data given in the table 1. The second set of data actually calculate a discrete time delay τ_0 , for which we get a Hopf bifurcation resulting in stable periodic solution. It is numerically observed that with proper choice of drug efficacies, hepatitis C virus can be controlled. Please note that a Hopf bifurcation was not found in a realistic parameter space with data set 1 but with data set 2, our analytical finding on the existence of a hopf bifurcation with biologically realistic parameters remain true. In the future, we would like to extend this work for different types of delays such as distributed delays or multiple discrete delays. Also, there are many components in this model that may be regarded as stochastic rather than deterministic and these variations may significantly alter the dynamics of the system. We, therefore, suggest to convert the system given by (2.2) into a stochastic delay differential equations and study its dynamics, which we propose as our future work.

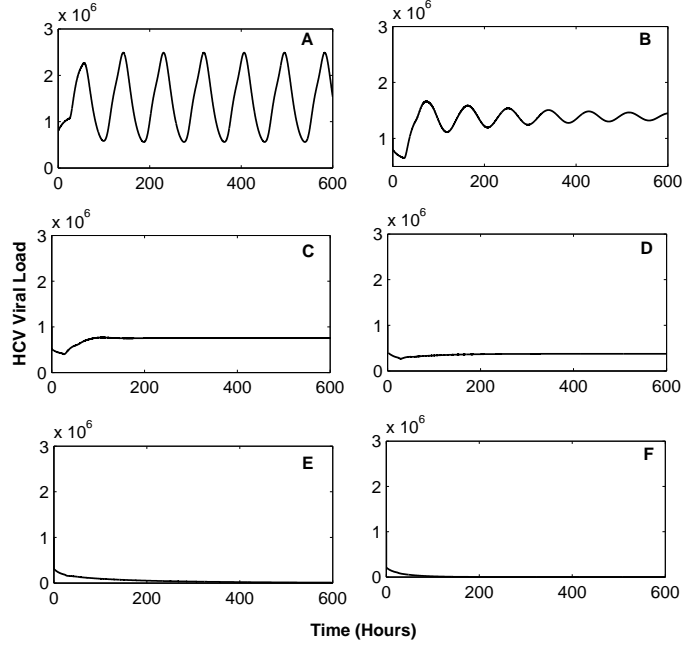


FIG. 4.7. The figure shows the dynamics of hepatitis C virus with intracellular delay $\tau = 24.1$ hours ($= \tau_0$), $\eta_1 = 0.5$, $\eta_r = 0.7$, $c = 0.81$, where the system exhibits Hopf bifurcation. As η_r is increased to 0.75, 0.8, 0.85, 0.9 and 0.95, decline in viral load has been observed (B, C, D, E, F). All the parameter values are taken from Table 2.

Appendix: Calculation of $W_{20}(\theta)$ and $W_{11}(\theta)$. From (3.27) and (3.29), we have

$$(5.1) \quad \dot{W} = \dot{x}_t - \dot{z}q - \dot{\bar{z}}\bar{q} = \begin{cases} AW - 2\text{Re}\{\bar{q}^*(0)f_0q(\theta)\}, & \text{if } \theta \in [-1, 0), \\ AW - 2\text{Re}\{\bar{q}^*(0)f_0q(0)\} + f_0, & \text{if } \theta = 0, \end{cases}$$

$$= AW + H(z, \bar{z}, \theta) \quad (\text{say}),$$

where

$$(5.2) \quad H(z, \bar{z}, \theta) = H_{20}(\theta)\frac{z^2}{2} + H_{11}(\theta)z\bar{z} + H_{02}(\theta)\frac{\bar{z}^2}{2} + \dots$$

Substituting the corresponding series into (5.1) and comparing the coefficients, we obtain

$$(5.3) \quad (A - 2i\tau_0\omega_0)W_{20}(\theta) = -H_{20}(\theta), AW_{11}(\theta) = -H_{11}(\theta), \dots$$

From (5.1), we know that for $\theta \in [-1, 0)$,

$$(5.4) \quad H(z, \bar{z}, \theta) = -\bar{q}^*(0)f_0q(\theta) - q^*(0)\bar{f}_0\bar{q}(\theta) = -g(z, \bar{z})q(\theta) - \bar{g}(z, \bar{z})\bar{q}(\theta).$$

Comparing the corresponding coefficients with that of (5.2), we get,

$$(5.5) \quad H_{20}(\theta) = -g_{20}q(\theta) - \bar{g}_{02}\bar{q}(\theta), H_{11}(\theta) = -g_{11}q(\theta) - \bar{g}_{11}\bar{q}(\theta).$$

From (5.3), (5.5) and the definition of A , it follows that

$$\dot{W}_{20}(\theta) = 2i\omega_0\tau_k W_{20}(\theta) + g_{20}(\theta)q(\theta) + \bar{g}_{02}\bar{q}(\theta).$$

Note that $q(\theta) = (1, a, b, c_1)^T e^{i\omega_0\tau_j\theta}$, hence

$$(5.6) \quad W_{20}(\theta) = \frac{ig_{20}}{\omega_0\tau_j} q(0)e^{i\omega_0\tau_j\theta} + \frac{i\bar{g}_{02}}{3\omega_0\tau_j} \bar{q}(0)e^{-i\omega_0\tau_j\theta} + E_1 e^{2i\omega_0\tau_j\theta},$$

Here $E_1 = (E_1^{(1)}, E_1^{(2)}, E_1^{(3)}, E_1^{(4)}) \in \mathbb{R}^4$ is a constant vector. Similarly, from (5.3) and (5.6), we get

$$(5.7) \quad W_{11}(\theta) = -\frac{ig_{11}}{\omega_0\tau_j} q(0)e^{i\omega_0\tau_j\theta} + \frac{i\bar{g}_{11}}{3\omega_0\tau_j} \bar{q}(0)e^{-i\omega_0\tau_j\theta} + E_2,$$

where $E_2 = (E_2^{(1)}, E_2^{(2)}, E_2^{(3)}, E_2^{(4)}) \in \mathbb{R}^4$ is also a constant vector. Now, we have to find an appropriate constant vector E_1 and E_2 which satisfy the above conditions. From the definition of A and (5.3), we obtain

$$(5.8) \quad \int_{-1}^0 d\eta(\theta) W_{20}(\theta) = 2i\omega_0\tau_j W_{20}(\theta) - H_{20}(\theta),$$

and

$$(5.9) \quad \int_{-1}^0 d\eta(\theta) W_{11}(\theta) = -H_{11}(0),$$

where $\eta(\theta) = \eta(0, \theta)$. Using (5.1), we have

$$(5.10) \quad H_{20}(0) = -g_{20}q(0) - \bar{g}_{20}\bar{q}(0) + 2\tau_j \begin{pmatrix} -(1+a)\frac{r}{T_{max}} - (1-c\eta_1)\alpha be^{-2i\omega_0\tau_j} \\ (1-c\eta_1)\alpha be^{-2i\omega_0\tau_j} \\ 0 \\ 0 \end{pmatrix}$$

and

$$(5.11) \quad H_{11}(0) = -g_{11}q(0) - \bar{g}_{11}\bar{q}(0) + 2\tau_j \begin{pmatrix} -(1+Re(a))\frac{r}{T_{max}} - (1-c\eta_1)\alpha Re(b) \\ (1-c\eta_1)\alpha Re(b) \\ 0 \\ 0 \end{pmatrix}$$

Substituting (5.6) and (5.10) into (5.8), we obtain

$$\left(2i\omega_0\tau_j I - \int_{-1}^0 e^{2i\omega_0\tau_j\theta} d\eta(\theta) \right) E_1 = 2\tau_j \begin{pmatrix} -(1+a)\frac{r}{T_{max}} - (1-c\eta_1)\alpha be^{-2i\omega_0\tau_j} \\ (1-c\eta_1)\alpha be^{-2i\omega_0\tau_j} \\ 0 \\ 0 \end{pmatrix}$$

which leads to

$$\begin{pmatrix} i\omega_0 - F & \frac{rT^*}{T_{max}} & (1 - c\eta_1)\alpha T^* & 0 \\ -(1 - c\eta_1)\alpha V_I^* e^{-i\omega_0\tau_j} & i\omega_0 + d_2 & -(1 - c\eta_1)\alpha T^* e^{-i\omega_0\tau_j} & 0 \\ 0 & -\left(1 - \frac{\eta_r + \eta_1}{2}\right)\beta & i\omega_0 + d_3 & 0 \\ 0 & -\left(\frac{\eta_r + \eta_1}{2}\right)\beta & 0 & i\omega_0 + d_3 \end{pmatrix} \begin{pmatrix} E_1^{(1)} \\ E_1^{(2)} \\ E_1^{(3)} \\ E_1^{(4)} \end{pmatrix} \\
= 2 \begin{pmatrix} -(1 + a)\frac{r}{T_{max}} - (1 - c\eta_1)\alpha b e^{-2i\omega_0\tau_j} \\ (1 - c\eta_1)\alpha b e^{-2i\omega_0\tau_j} \\ 0 \\ 0 \end{pmatrix}$$

From above, we can easily calculate a constant vector $E_1 = (E_1^{(1)}, E_1^{(2)}, E_1^{(3)}, E_1^{(4)}) \in R^4$. Similarly, substituting (5.7) and (5.11) into (5.9), we can get

$$\begin{pmatrix} F & -\frac{rT^*}{T_{max}} & -(1 - c\eta_1)\alpha T^* & 0 \\ -(1 - c\eta_1)\alpha V_I^* & -d_2 & -(1 - c\eta_1)\alpha T^* & 0 \\ 0 & \left(1 - \frac{\eta_r + \eta_1}{2}\right)\beta & -d_3 & 0 \\ 0 & \left(\frac{\eta_r + \eta_1}{2}\right)\beta & 0 & -d_3 \end{pmatrix} \begin{pmatrix} E_2^{(1)} \\ E_2^{(2)} \\ E_2^{(3)} \\ E_2^{(4)} \end{pmatrix} \\
= 2 \begin{pmatrix} -(1 + Re(a))\frac{r}{T_{max}} - (1 - c\eta_1)\alpha Re(b) \\ (1 - c\eta_1)\alpha Re(b) \\ 0 \\ 0 \end{pmatrix}$$

In the similar manner, we can calculate the constant vector $E_2 = (E_2^{(1)}, E_2^{(2)}, E_2^{(3)}, E_2^{(4)}) \in R^4$.

Acknowledgments. This study was supported by Initiation Grant (Grant number IITR/SRIC/100518) from the Indian Institute of Technology Roorkee, Roorkee, India.

REFERENCES

- [1] P. BACCAM, C. BEAUCHEMIN, C. A. MACKEN, F. G. HAYDEN, AND A. S. PERELSON, *Kinetics of influenza A virus infection in humans*, Journal of Virology, 80 (2006), pp. 7590 – 7599.
- [2] SANDIP BANERJEE AND RAM KEVAL AND SUNITA GAKKHAR, *Modeling the dynamics of Hepatitis C virus with combined antiviral drug therapy: Interferon and Ribavirin*, Mathematical Biosciences, 245 (2013), pp. 235 – 248.
- [3] F.C. BEKKERING, J.T. BROUWER, G. LEROUX-ROELS, H. VAN VLIERBERGHE, A. ELEWAUT AND S.W. SCHALM, *Ultrarapid hepatitis C virus clearance by daily high-dose interferon in non-responders to standard therapy*, Journal of Hepatology, 28(6) (1998), pp. 960–964.
- [4] F.C. BEKKERING, J.T. BROUWER, S. SCHALM AND A. ELEWAUT, *Hepatitis C: viral kinetics*, Hepatology, 26(6) (1997), pp. 1691–1693.
- [5] H.C. BODENHEIMER JR, K.L. LINDSAY, G.L. DAVIS, J.H. LEWIS, S.N. THUNG AND L.B. SEEFF, *Tolerance and efficiency of oral ribavirin treatment of chronic hepatitis C: a multitrial*, Hepatology, 26(2) (1997), pp. 473–477.
- [6] S. P. CHAKRABARTY AND H. R. JOSHI, *Optimally controlled treatment strategy using interferon and ribavirin for hepatitis C*, Journal of Biological Systems, 17 (2009), pp. 97 – 110.
- [7] K. COOKE AND P. VAN DEN DRIESSCHE, *On zeroes of some transcendental equations*, Funkcialaj Ekvacioj, 29 (1986), pp. 77–90.
- [8] REBECCA V. CULSHAW AND SHIGUI RUAN, *A delay-differential equation model of HIV infection of CD4+ T-cells*, Mathematical Biosciences, 165 (2000), pp. 27–39.
- [9] H. DAHARI, E. S. A. D. ARAUJO, B. L. HAAGMANS, T. J. LAYDEN, S. J. COTLER, A. A. BARONE AND A. U. NEUMANN, *Pharmacodynamics of PEG-IFN- α -2a in HIV/HCV co-infected patients: Implications for treatment outcomes*, Journal of Hepatology, 53 (2010), pp. 460–467.

- [10] H. DAHARI, A. LO, R. M. RIBEIRO, AND A. S. PERELSON, *Modeling hepatitis C virus dynamics: Liver regeneration and critical drug efficacy*, Journal of Theoretical Biology, 247 (2007), pp. 371 – 381.
- [11] A.M. DI BISCEGLIE, H.S. CONJEEVARAM, M.W. FRIED, R. SALLIE, Y. PARK, C. YURDAYDIN, M.G. SWAIN, D.E. KLEINER, K. MAHANEY AND J.H. HOOFNAGLE, *Ribavirin as therapy for chronic hepatitis C. A randomized, double-blind, placebo-controlled trial*, Annals of Internal Medicine, 123(12) (1995), pp. 897-903.
- [12] A.M. DI BISCEGLIE, M. SHINDO, T.L. FONG, M.W. FRIED, M.G. SWAIN, N.V. BERGASA, C.A. AXIOTIS, J.G. WAGGONER, Y. PARK AND J.H. HOOFNAGLE, *A pilot study of ribavirin therapy for chronic hepatitis C*, Hepatology, 16(3) (1992), pp. 649–654.
- [13] J. DIEUDONNÉ, *Foundations of Modern Analysis* (1960), Academic Press, New York,
- [14] N. M. DIXIT, *Advances in the Mathematical Modelling of Hepatitis C Virus Dynamics*, Journal of Indian Institute of Science, 88(2008), pp. 37 – 43.
- [15] N. M. DIXIT, J. E. LAYDEN-ALMER, T. J. LAYDEN, AND A. S. PERELSON, *Modelling how ribavirin improves interferon response rates in hepatitis C virus infection*, Nature, 432 (2004), pp. 922 – 924.
- [16] N. M. DIXIT, AND A. S. PERELSON, *Complex patterns of viral load decay under antiretroviral therapy: influence of pharmacokinetics and intracellular delay*, Journal of Theoretical Biology, 226 (2004), pp. 95 - 109
- [17] N. M. DIXIT AND A. S. PERELSON, *HIV dynamics with multiple infections of target cells*, PNAS USA, 102 (2005), pp. 8198 – 8203.
- [18] J. J. FELD AND J. H. HOOFNAGLE, *Mechanism of action of interferon and ribavirin in treatment of hepatitis C*, Nature, 436 (2005), pp. 967 – 972.
- [19] H. FREEDMAN, AND V. S. H. RAO, *The trade-off between mutual interference and time lags in predator-prey systems*, Bulletin Mathematical Biology, 45 (1983), pp. 991 – 1004.
- [20] S. A. GOURLEY, Y. KUANG, AND J. D. NAGY, *Dynamics of a delay differential equation model of hepatitis B virus infection*, Journal of Biological Dynamics, 2 (2008), pp. 140 – 153.
- [21] J. D. GRACI AND C. E. CAMERON, *Mechanisms of action of ribavirin against distinct viruses*, Rev Med Virol, 16 (2006), pp. 37 – 48.
- [22] J. G. GUATELLI, T. R. GINGERAS AND D. D. RICHMAN, *Alternative splice acceptor utilization during human immunodeficiency virus type 1 infection of cultured cells*, Journal of Virology, 64 (1990), pp. 4093 - 4098.
- [23] B. D. HASSARD, N. D. KAZARINIFF, AND Y. H. WAN, *Theory and applications of Hopf bifurcation*, London math society lecture note series, 41 (1981), Cambridge University Press.
- [24] E. HERRMANN, J.H. LEE, G. MARINOS, M. MODI AND S. ZEUZEM, *Effect of ribavirin on hepatitis C viral kinetics in patients treated with pegylated interferon*, Hepatology, 37 (6) (2003), pp. 1351-1358.
- [25] N.P. LAM, A.U. NEUMANN, D.R. GRETCH, T.E. WILEY, A.S. PERELSON AND A.J. LAYDEN, *Dose dependent acute clearance of hepatitis C genotype1 virus with interferon alpha*, Hepatology, 26(1) (1997), pp. 226–231.
- [26] J.E. LAYDEN-ALMER AND R.M. RIBEIRO AND T. WILEY AND A.S. PERELSON AND T.J. LAYDEN, *Viral dynamics and response differences in HCV infected African American and white patients treated with IFN and ribavirin*, Hepatology, 37 (6) (2003), pp. 1343–1350.
- [27] S. R. LEWIN, R. M. RIBEIRO, T. WALTERS, G. K. LAU, S. BOWDEN, S. LOCARNINI, AND A. S. PERELSON, *Analysis of hepatitis B viral load decline under potent therapy: complex decay profiles observed*, Hepatology, 34 (2001), pp. 1012 – 1020.
- [28] P. W. NELSON AND A. S. PERELSON, *Mathematical analysis of delay differential equations models of HIV-1 infection*, Mathematical Biosciences, 179 (2002), pp. 73 – 94.
- [29] A. U. NEUMANN, N. P. LAM, H. DAHARI, D. R. GRETCH, T. E. WILEY, T. J. LAYDEN, AND A. S. PERELSON, *Hepatitis C Viral Dynamics in Vivo and the Antiviral Efficacy of Interferon- α Therapy*, Science, 282 (1998), pp. 103 – 107.
- [30] M. A. NOWAK, S. BONHOEFFER, A. M. HILL, R. BOEHME, H. C. THOMAS, AND H. MCDADE, *Viral dynamics in hepatitis B virus infection*, PNAS USA, 93 (1996), pp. 4398 – 4402.
- [31] J.M. PAWLOTSKY, H. DAHARI, A.U. NEUMANN, C. HEZODE, G. GERMANIDIS, I. LONJON, L. CASTERA AND D. DHUMEAUX, *Antiviral action of ribavirin in chronic hepatitis C*, Gastroenterology, 126 (3) (2004), pp. 703–714.
- [32] A. S. PERELSON AND P. W. NELSON, *Mathematical Models of HIV-Dynamics in vivo*, SIAM Review, 41 (1999), pp. 3 – 44.
- [33] F. RIESZ, *Sur une espèce de géométrie analytique des systèmes de fonctions sommables*, Comptes rendus de l'Académie des sciences Paris, 144 (1907), pp. 1409–1411.
- [34] S. ZEUZEM, J.M. SCHMIDT, J.H. LEE, M. VON WAGER, G. TEUBAR AND W.K. ROTH, *Hepatitis C virus dynamics in vivo: effect of ribavirin and inteferon alpha on viral turnover*,

Hepatology, 28(1) (1998), pp. 245–252.